XIV ConvegnoNazionale A.I.VE.LA.
Roma, 6-7 Novembre 2006

PIV analysis around the Bilge Keel of a Ship Model in Free Roll Decay

G.Aloisio[*], F.Di Felice [*].

[*] **INSEAN, Italian Ship Model Basin, Rome**

Abstract

The results of an experimental analysis of the velocity field around a ship model in forced roll motion are presented. Tests, carried out at the INSEAN towing tank n° 2, aim to achieve a better physical understanding of the fluid dynamics and a certified experimental data set for CFD validation. Results describe the evolution of the flow field in two cross sections along the bilge keels during damped roll motion. A PIV algorithm based on window deformation is used to improve the estimate of the vorticity. The mean unsteady flow field is obtained by ensemble averaging of time histories. The hydrodynamic damping effectiveness of the bilge keels is highlighted by the generation of strong vortical structures that characterize the transfer of energy between the hull and the surrounding flow field.

1 Introduction

Motion prediction of a ship in seaway is a complex task and is one of the main topics in today's hydrodynamic research. Whereas, for most degrees of freedom, a small amount of information on the ship geometry and on the sea state are sufficient to predict the response of the ship, the roll motion is particularly difficult to estimate. Roll is, in fact, a lightly damped and lightly restored motion and the roll natural period of the conventional ship is very close to the richest region in the wave energy spectrum. Very large amplitude of the roll motion can then occur, even in moderate sea state, if the wave frequency spectrum is narrow and tuned with the ship roll natural period. In even more moderate conditions, the roll motion is of concern, since undesirable effects may arise from excessive lateral accelerations. Ship capsizing is the extreme consequence of this phenomenon.

From the theoretical point of view, the prediction of the roll motion is a challenging task: it is governed by the viscous effect and the damping is mainly induced by the vortex shedding phenomena. The Navier Stokes equation is the mathematical model able to reproduce the hydrodynamic field around the hull in roll motion. The difficulties in predicting the roll damping of a ship depend not only on the nonlinear characteristics of the phenomenon but also on its strong dependence upon the presence or not of bilge keels and upon the forward speed of the ship. The flow separation due to a ship bilge keel significantly affects the evolution of the roll motion. Therefore, the analysis of the induced vortical structures and their evolution with the roll angle, as well as the evaluation of forces and moments applied to the ship during the roll motion, are of primary relevance to the dynamics of the ship. The difficulty of implementing this kind of model explains the strong development of the empirical methods (Ikeda et al. 1978; Himeno 1981).

From the numerical point of view, simulations based on 2D viscous flow mathematical models (Yeung et al. 1998; Roddier et al. 2000) have been extensively used in the past. Recently, simulations of increasingly complex ship 3D flows have been performed (Broglia et al, 2003; Di Mascio et al. 2004). For the development and the validation of CFD codes, much more detailed model-scale, surface ship experimental data is required. Official issues from ITTC' 1999 and 2003 require explicitly EFD and CFD to be more and more interlaced in order to provide reliable tools for a better understanding of fluid physics. Experimental works for validating theoretical and

G.Aloisio, F. Di Felice INSEAN (Italian Ship Model Basin), Via di Valleranno 139, 00128 Rome, Italy

Correspondence to:
Giovanni Aloisio,
INSEAN, Propulsion and Cavitation Group, Via di Valleranno 139, 00128 Rome Italy email; g.aloisio@insean.it

numerical models have been performed (Yeung et al. 1996). Recently, Felli et al (2004) performed LDV measurements for a frigate model in forced roll motion. The influence of several appendages on the motion and on the flow field evolution around the hull was investigated.

In the present work an experimental investigation of the velocity field evolution around the bilge keels of a ship model in free decay roll motion is presented and discussed. The present work has been performed in cooperation with the David Taylor Model Basin (Bishop et al. 2004).and the University of Iowa (Irvine et al. 2004).

2 Experimental Setup

The experiments were carried out at the INSEAN towing tank n°2. The tank is 250 m long, 9 m wide and 4.5 m deep, with a maximum carriage speed of 10 m/s. More information regarding the facility capabilities can be found at http://www.insean.it.

A 5720 mm length frigate model (INSEAN model C2340) with bilge keels is tested. A sketch of the experimental set-up is shown in figure 1.

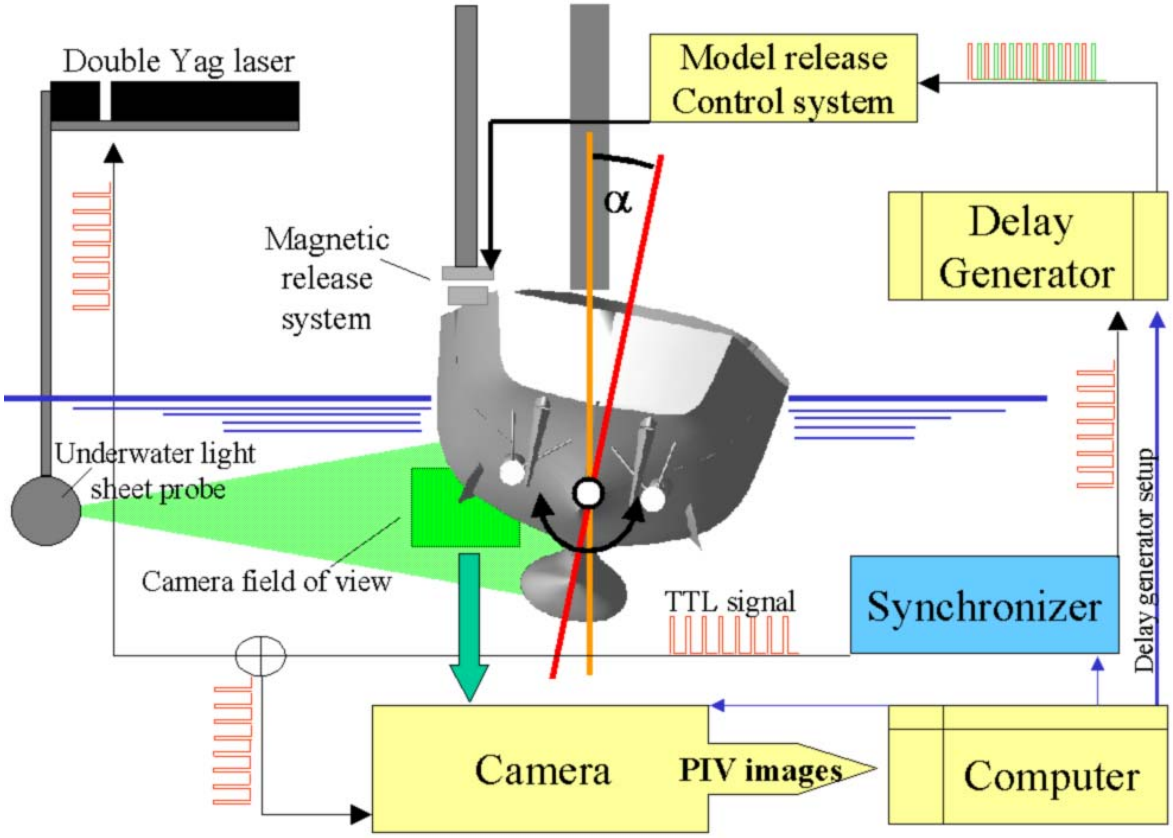

Figure 1: Experimental setup

The light sheet, generated by a two-head Nd-YAG laser, was delivered to the measurement plane by means of underwater optics. The laser light sheet pulse rate was 12.5 Hz, with an energy output of 200 mJ per pulse. 2D PIV measurements were performed by using an underwater camera with a 1280X1024 pixel^2 resolution. Roll being the only motion allowed in this experiment, the ship model was locked to the dynamic trim at an initial roll angle of 10° by means of a magnet. A TTL trigger sequence was generated by a synchronizing device to pilot the Nd–YAG lasers and the camera acquisition system. The first pulse of this sequence would deactivate the magnet, thus releasing the model and starting the roll cycle and the image recording sequence.

The maximum acquisition frequency was 3 Hz, due to the limitation of the image acquisition bandwidth. This was not sufficient to resolve in time the flow field evolution of the damped roll motion, which had a natural

frequency of about 0.5 Hz. In order to obtain a mean evolution of the unsteady flow, each run has been repeated several times with a varying start delay. By using a delay generator between the synchronizer and the magnet-based release control system, it was possible to change the time interval between the start of the acquisition sequence and the model release. Hence, the flow field evolution was sampled at different roll angles by scanning the free decay time history four times and using a delay of 1/12 sec between two consecutive acquisitions as shown in figure 2. This procedure allowed a final reconstruction of the ensemble averaged flow field at a final sampling rate of 12 Hz. For each roll angle, 64 PIV measurements have been performed to evaluate the ensemble mean flow.

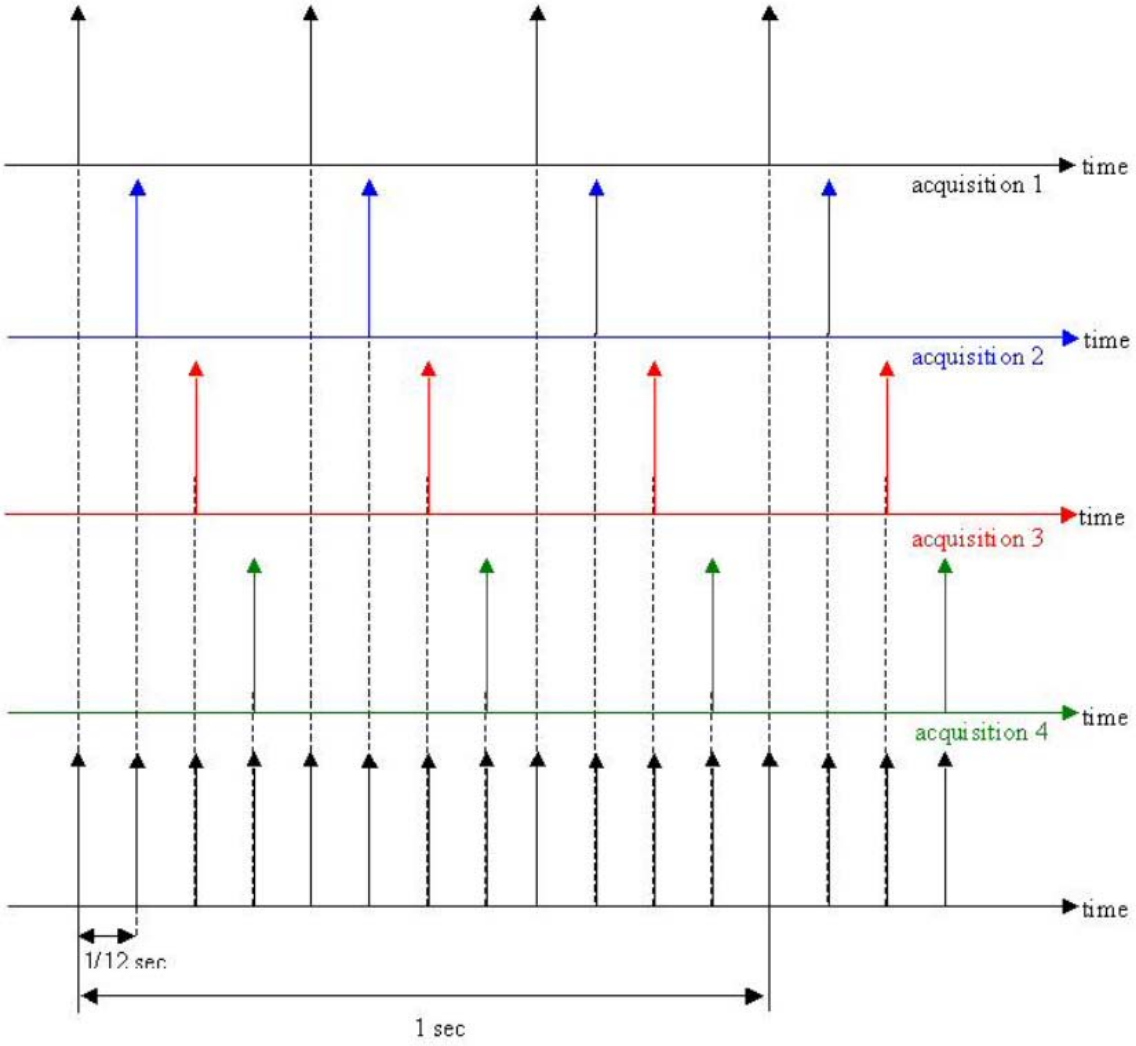

Figure 2: time sequences used for the reconstruction of the mean flow time history

Measurements were performed along 2 transversal sections of the hull, at x/L=0.504 (plane 1) and x/L=0.675 (plane 2) from the PPAV, L being the model length. Measurements at plane 1 were performed both at Froude number Fr=0 and Fr=0.138 for an initial roll angle of 10°. Plane 2 was measured at Fr=0.138 only, with an initial roll angle of -10°.

The time evolution of the angular position of the rolling body was acquired simultaneously with the velocity time history, as shown in figures 3 and 4. A high repeatability of the roll angle evolution could be verified, allowing a quick convergence of the ensemble statistics. The flow evolution corresponding to Fr=0.138 was reconstructed up to the first 5 cycles, while a longer sequence of 10 cycles was considered for Fr=0 due to a weaker motion damping.

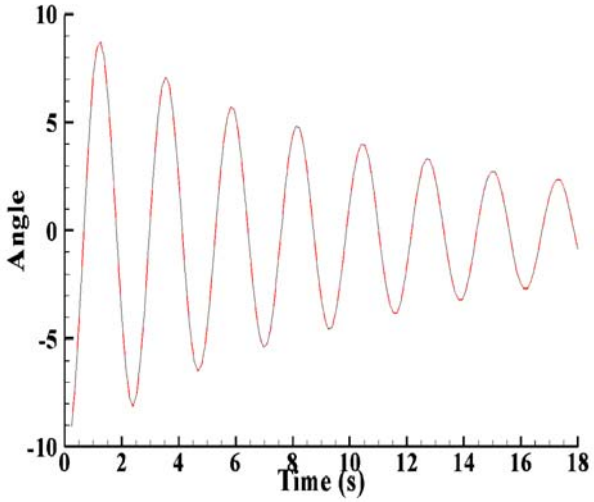

Figure 3: Roll angle time history for Fr=0

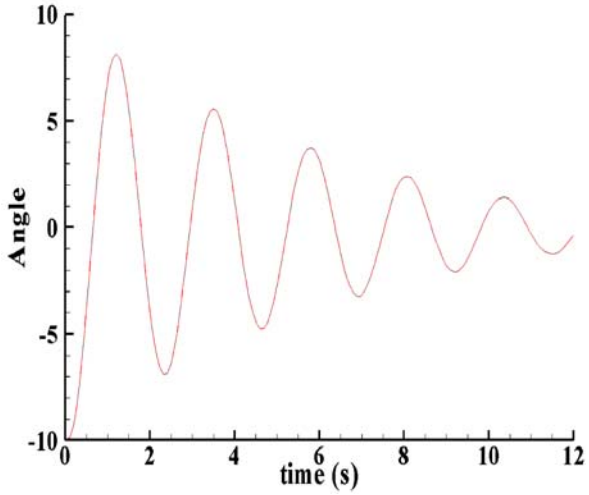

Figure 4: Roll angle time history for Fr=0.138

In order to improve the quality of the images the water was seeded with 10-μm hollow glass spheres. The seeding rake was located downstream the model and the flow seeded during the returning tow to avoid upstream flow disturbances during the test.

3
Image Analysis

PIV analysis was performed combining the discrete offset technique and the iterative image deformation method (Di Florio et al 2002). The displacement field obtained with the first analysis method was used to distort the images (Huang et al 1993), upon which direct cross-correlation was applied to calculate a "corrected" velocity field. This newly updated velocity predictor was subsequently used to re-distort the original images and the process was repeated on an iterative basis until a convergence criterion could be verified. This type of iterative algorithm has been recently proved to be very efficient, accurate and stable (Scarano and Riethmuller 2000, Scarano 2002). Tests made on synthetic images showed that both the mean displacement error and the rms error were reduced by about one order of magnitude. The maximum measurable gradient was also found to increase, hence making possible the measurement of velocities in a dynamic range 1.5 to 2.5 orders of magnitude larger than with the standard PIV analysis. As a direct consequence, the vorticity peak levels were equally enhanced and closer to actual values. This improvement is very important for the correct detection of the vortex cores and of the shear regions generated by the bilge keels. In the general case, it allows for the correct evaluation of velocity in cross flow measurements where the predominant out-of-plane velocity component requires very small time intervals between PIV frames, thus concentrating the displacement information in the subpixel range where errors tend to be important.

The processing set-up used in this case was composed by a 3-step discrete offset method with a final window size of 28x28 pixel^2 and a grid spacing between the vectors of 10 pixels (i.e. 65% overlap). The image deformation was then performed through 4 iterations with a local Gaussian weighting filter applied to the predictor field and a Gaussian sub-pixel interpolation fit.

4

Results

In this section, the velocity fields relative to two different Froude numbers, Fr=0 and Fr=0.138, will be presented and discussed. As already stated, the flow in two different planes will be investigated for Fr=0.138 in order to highlight some aspects of the time history of the vorticity in the longitudinal direction, and to evaluate the effect of the bilge keels along the hull.

Fr=0

Due to the absence of forward speed, the roll damping contribution is small and it is mainly induced by the vorticity shedding from the bilge keels at each cycle. This behavior is well highlighted in figure 5, where the evolution of the vorticity during the first two cycles of the free decay roll motion is shown. The vortex shedding occurs in vortex packets with a spatial frequency proportional to the angular acceleration of the bilge keels. In particular, the vorticity field reproduces the well known Kelvin-Helmholtz instability, already pointed out from numerical simulations by Koumoutsakos (1996) for a flat plate uniformly accelerated and characterized by a non-dimensional parameter $\alpha = \dot{V} b^3 / \nu^2$ larger than $2 \cdot 10^5$, with *b* being the dimension of the plate, $\dot{V}$ the acceleration and ν the cinematic viscosity. In the present case, respectively assuming the height *h* of the bilge keel and the maximum acceleration $\dot{\vartheta}\, h$ at the tip of the bilge keel as the characteristic geometrical length and acceleration, the parameter $\alpha = \dot{\vartheta} h^4 / \nu^2$ takes a value of $4.4 * 10^6$.

The vortex packet is rolled up in a large vortex whose intensity decreases with the amplitude of the roll motion with every new cycle. When the roll motion changes direction, two strong counter rotating vortices are simultaneously present. Their interaction is strong and they trust each other far from the hull. Expansion and energy diffusion of the vortex structures can be also highlighted as the free roll decay progresses in time. This physical effect is further amplified by the ensemble averaging process. During the successive cycles, in fact, the released vortices interact randomly with the previously generated flow structures causing a slightly different displacement for each cycle. This effect can be further confirmed by observing in figure 6 the growth in time of the turbulence level represented as the rms of the transversal component U; the vertical component V displays the same behavior. The vortex pair generated in the first cycle remains in the measurement region, see top left corner in figure 6, and adds up to the turbulence levels during the rest of the cycle, see row 3 columns 2, 3 and 4.

Fr=0.138

Measurements were performed at a speed of 1.024 m/s, corresponding to a Froude number of 0.138. The vorticity shedding time history is shown in figure 7. The forward speed of the ship produces strong modifications of the flow behavior: the advection of the vorticity along the direction perpendicular to the measurement plane takes place and a boundary layer in the longitudinal direction appears that interacts with the vorticity field and causes its diffusion. Shed vorticity reaches 50% higher values than the case at Fr=0, hence inducing a stronger damping, see figures 3 and 4. The instability previously observed at Fr=0 is not visible on the ensemble mean history. However, it has been observed in the instantaneous flow field, though with a random spacing that is therefore lost in the ensemble averaging process where it appears in the form of a shear layer. This randomness is caused by the ship model turbulent boundary layer.

At section x/L=0.504, the tip of the bilge keel emerges from the ship boundary layer, as seen on figure 8 where the fluctuations of the transversal component U are shown. As a consequence, the main vortices are lightly affected by the boundary layer and their diffusion starts essentially in the second cycle, where their intensity is lower. In contrast, the bilge keel at section x/L = 0.675 is completely immersed in the ship model boundary layer, whose thickness increases in the downstream direction as a consequence of the adverse pressure gradient therein experienced, see figure 9. This results in a faster diffusion of the bilge keel vortices and higher turbulence levels with respect to the upstream plane.

5
Conclusion

An experimental survey of the velocity field of a ship model in damped rolling motion was carried out. The flow around the bilge keels was investigated using a 2D PIV underwater system. The velocity field evolution during the damped motion has been reconstructed using ensemble averages.
The following conclusions can be pointed out:

- The vortex shedding is the main physical mechanism involved in the damping of the roll motion. The vorticity shed from the bilge keels is proportional to the amplitude of the motion.
- Release of vortex packets occurs at Fr=0. It is supposed that this packet release also occurs at Fr=0.138 as observed on the instantaneous velocity fields. In this latter situation, however, the ship turbulent boundary layer strongly disturbs the vortex shedding process, which therefore is not captured in the mean flow field reconstruction.
- Further downstream along the hull, the effect of the thicker ship boundary layer is enhanced and causes a faster diffusion of the vorticity and its quick advection toward the far field.

References

Bishop R., Atsvapranee P., Percivall S.,Shan J., Engle A. (2004) ”An Investigation of the Viscous Roll Damping Through the Application of Particle Image Velocimetry”, 25th Symposium on Naval Hydrodynamics, S. Johns, Newfoundland, Canada.
Broglia R., Di Mascio A. (2003) “Unsteady RANSE calculations of the fow around a moving ship hull”. 8th NSH Busan, Korea.
Di Florio G., Di Felice F., Romano G. P. (2002) “Windowing, re-shaping and reorientation interrogation windows in particle image velocimetry for the investigation of shear flows”, Measurement Sci. Technol. **13**, pp 953-962.
Di Mascio A., Broglia R., Muscari R., Dattola R. (2004) “Unsteady RANSE simulations of a manoeuvering ship hull”. 25th Symposium on Naval Hydrodynamics, S. Johns, , Newfoundland Canada
Felli M., Di Felice F., Lugni C. (2004) “Experimental study of the flow field around a rolling ship model“ 25th Symposium on Naval Hydrodynamics, S. John’s, Newfoundland, Canada.
Himeno Y. (1981) “Prediction of ship roll damping-state of art", Dept.of Naval Arch. And Marine Eng, Univ. of Michigan, Rep. No. 239.
Huang H. T., Fielder H. F., Wang J. J. (1993) “Limitation and improvement of PIV; part II: Particle Image Distortion, a novel technique” Exp. Fluids 15, pp. 263-273.
Ikeda Y., Himeno Y., Tanaka N.(1978) “A prediction method for ship roll damping”, Rep. No. 00405 of Dep. of Naval Arch., Univ. of Osaka.
Irvine M., Longo J., Stern F. (2004) ”Towing Tank Test for Surface Combatant for Free Roll Decay and Coupled Pitch and Heave Motion” 25th Symposium on Naval Hydrodynamics, S. Johns, , Newfoundland Canada.
Koumoutsakos P., Shiels D., (1996) “Simulations of the viscous flow normal to an impulsively started and uniformly accelerated flat plate” Journal of Fluid Mechanics 328: 177-227.
Roddier D., Liao S., Yeung R., (2000) “On Freely-Floating Cylinders fitted with bilge keels”, Proc. Int. Off. and Polar Eng. Conf., Seattle.
Scarano F., Riethmuller M. L. (2000) “Advances in Iterative Multigrid PIV Image Processing” Exp. Fluids, pp. 51-60.
Scarano F. (2002) “Iterative image deformation methods in PIV” Measurement. Sci. Technol. **13** pp. 1-19
Yeung R., Cermelli C., Liao S. (1996) “Vorticity fields due to Rolling Bodies in a Free Surface-Experiment and Theory”, 21st ONR Symposium, Trondheim, Norway.
Yeung R., Liao S., Roddier D. (1998) “On roll Hydrodynamics of Rectangular Cylinders”, Proc. Int. Off. and Polar Eng. Conf., Montreal.

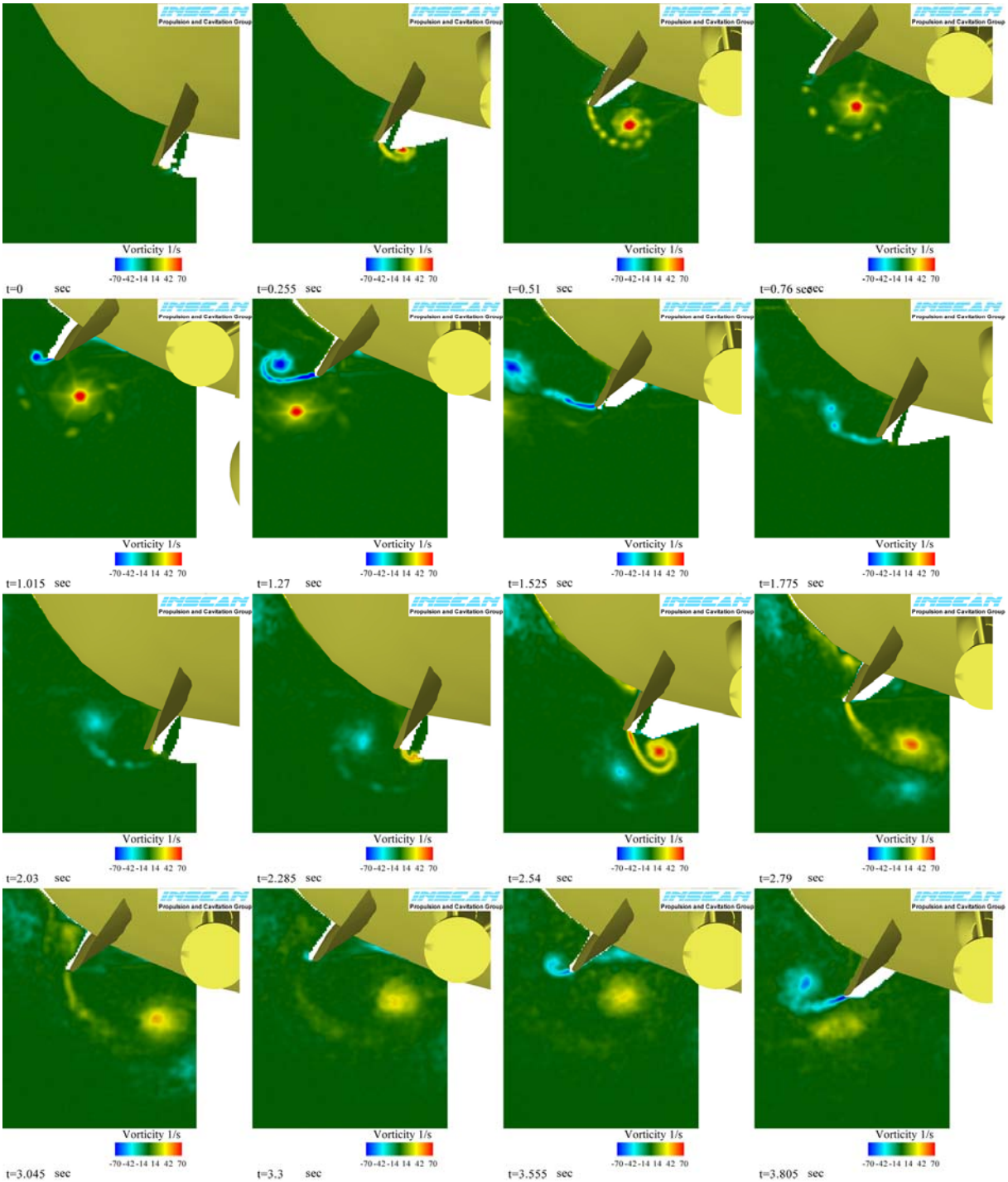

Figure 5: Vorticity evolution during the free roll decay; x/L=0.504, Fr=0

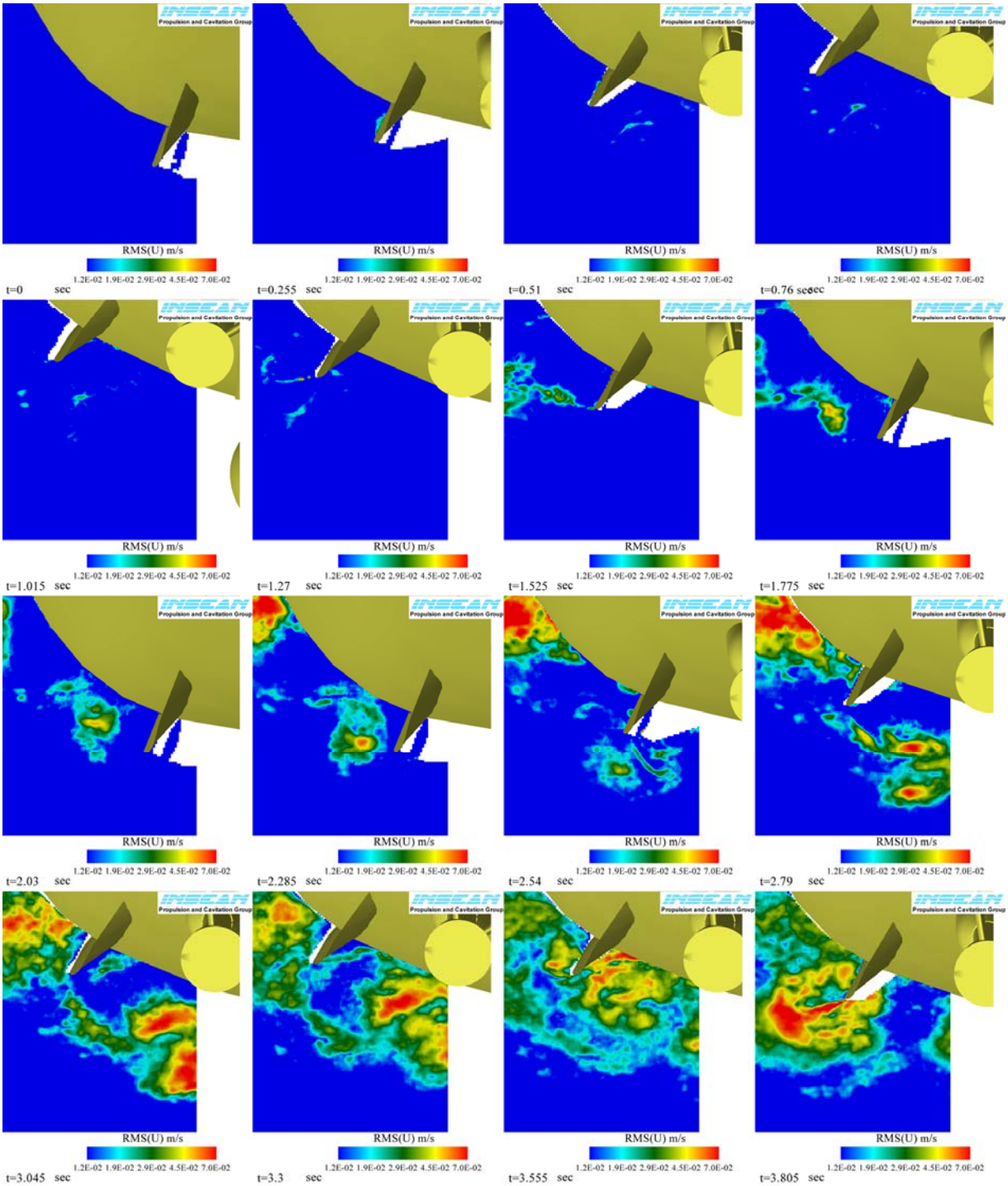

Figure 6: Transversal component (U) fluctuations during the free roll decay; x/L =0.504, Fr=0

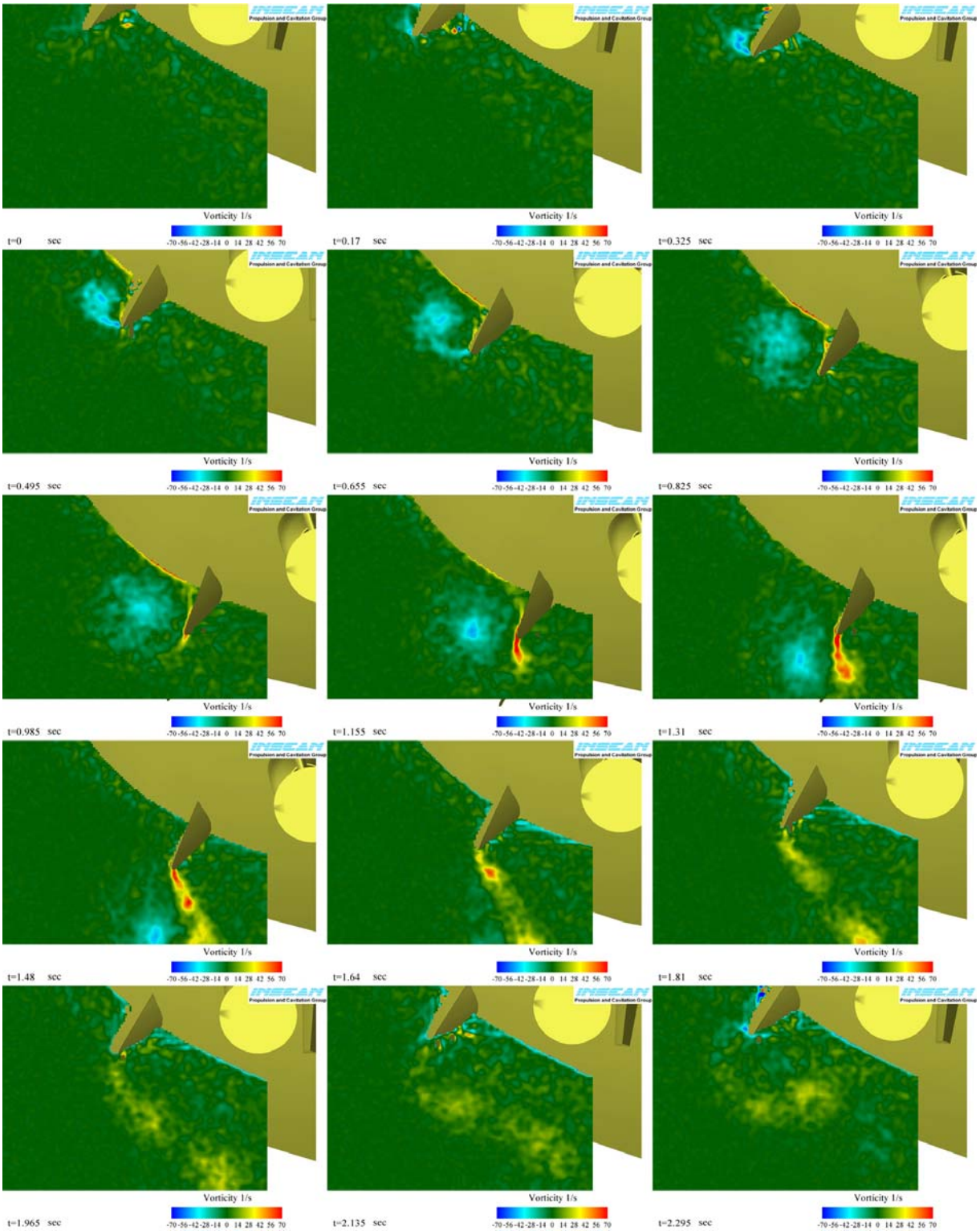

Figure 7: Vorticity evolution during the free roll decay; x/L=0.504, Fr=0.138

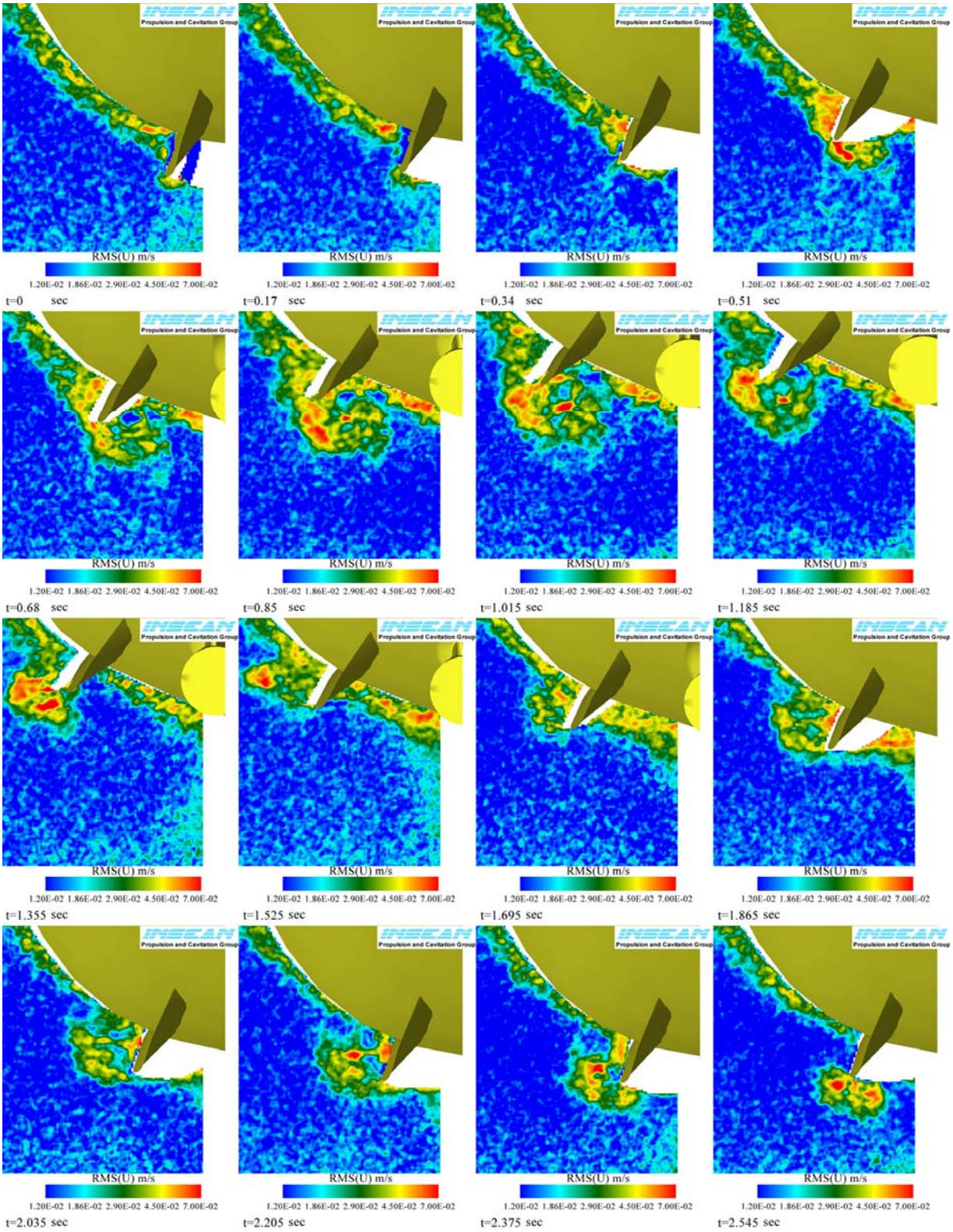

Figure 8: Transversal component (U) fluctuations during the free roll decay; x/L =0.504, Fr=0.138

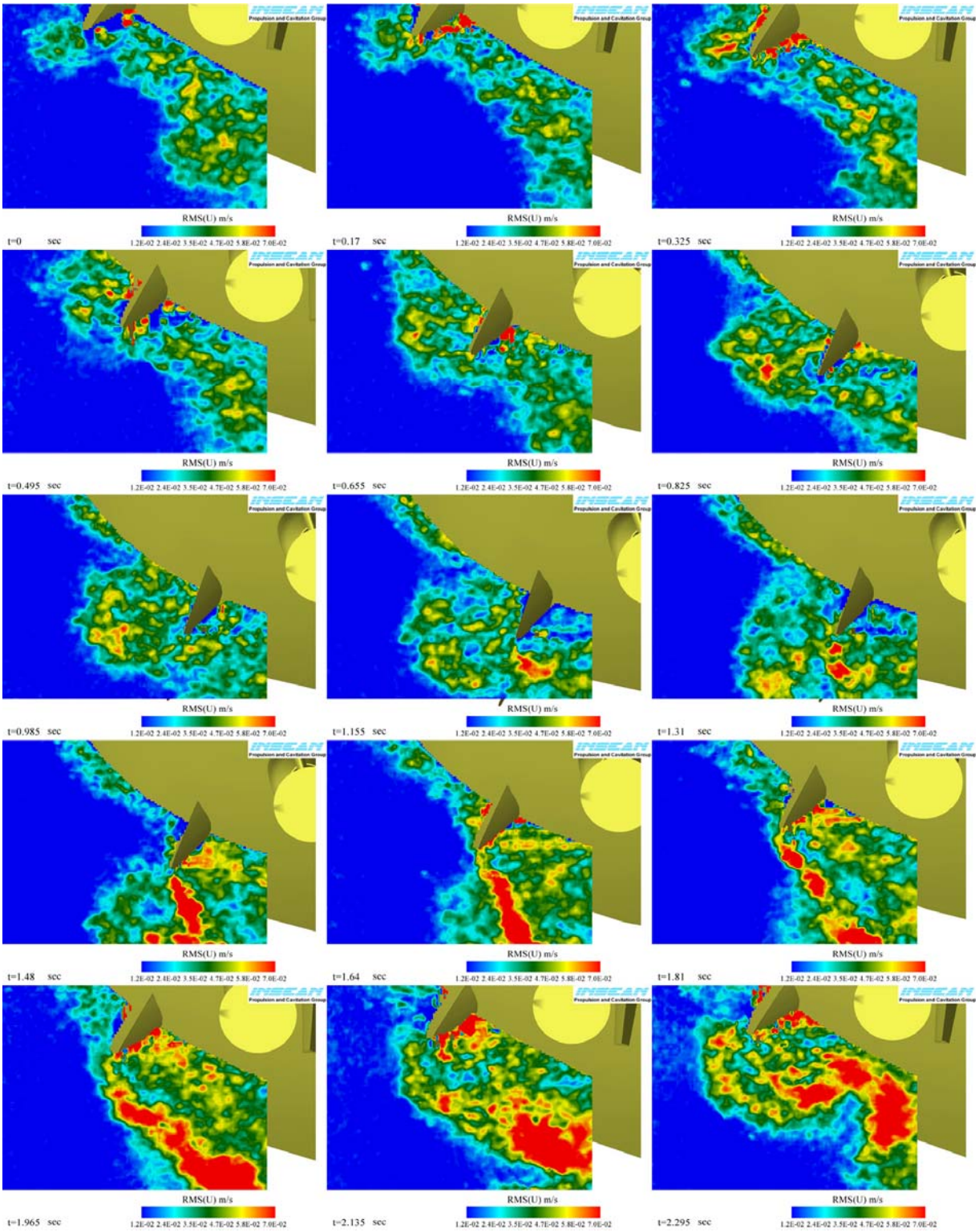

Figure 9: Transversal component (U) fluctuations during the free roll decay; x/L =0.675, Fr=0.138